Nuclear Materials and Energy xxx (xxxx) xxxx

Contents lists available at ScienceDirect

Nuclear Materials and Energy

journal homepage: www.elsevier.com/locate/nme

ColRadPy: A Python collisional radiative solver

C.A. Johnson*, S.D. Loch, D.A. Ennis

Auburn University, Auburn, AL 36849, United States of America

ARTICLE INFO

2010 MSC:
00-01
99-00

ABSTRACT

The properties of emitting ions in a plasma provides both potential for plasma diagnostics and key information required for plasma modeling. Generalized collisional radiative theory provides a powerful tool for the modeling of low and moderately dense plasmas. A new Python program is presented that solves the collisional radiative and ionization balance equations for application to fusion, laboratory, and astrophysical plasmas. It produces generalized coefficients that can be easily imported into existing plasma modeling codes and spectral diagnostics. An overview of the code is presented, along with selected results for applications to high-Z plasma facing components.

1. Introduction

Collisional Radiative (CR) theory was originally developed by Bates, Kingston, and McWhirter [1] and was later generalized to include the role of metastable states (see the review article by Summers et al. [2]). Generalized collisional radiative theory has been successful at accurately modeling both astrophysical [3] and laboratory plasmas [4]. This method produces a set of atomic parameters known as Generalized Collisional Radiative (GCR) coefficients that are convenient for use in plasma modeling codes [5].

In this paper, a brief review of generalized collisional radiative theory is presented and then a new Python code that has been developed (ColRadPy) will be described. A number of other collisional radiative codes exist, including those in the ADAS suite of codes [6], the CHIANTI suite of codes [7] and atomDB [8]. The purpose of the newly developed code that is presented here is to provide a convenient Python model that can be incorporated into other Python codes. This code is designed to take ADAS formatted data input files and produce standard ADAS output files as well as to hold the results in Python arrays.

In the next section, a theoretical description of the collisional radiative equations and the GCR coefficients will be presented. Section 3 compares ColRadPy with the widely used and tested ADAS suite of codes. Section 4 gives example applications of ColRadPy for neutral molybdenum and neutral beryllium.

2. Review of generalized collisional radiative theory

2.1. Excited populations and emissivity

Generalized collisional theory balances the rate equations for populations of ground, metastable, and excited states. The atomic processes that impact the rate equations include: electron impact excitation/de-excitation (q), electron impact ionization (S), electronic recombination (including radiative recombination, dielectronic recombination and three body recombination) (R), and spontaneous emission (A). There are additional possible process that become important for particular applications e.g. (charge exchange) that are not discussed here. The terms in parentheses indicate the variables assigned for these processes in the paper. All of these processes have been described in detail elsewhere [2]. We illustrate electron impact excitation/de-excitation and spontaneous emission below.

Electron impact excitation occurs when the energy state of an impurity atom is increased due to the interaction with a free electron Eq. (1) where X^{+Z} is the impurity atom and e is the electron with the ϵ denoting the energy of the state.

$$X^{+Z}(i) + e(\epsilon_n) \leftrightarrow X^{+Z}(j) + e(\epsilon_m) \tag{1}$$

Spontaneous emission occurs when an electron decays from a higher to lower energy state Eq. (2) and emits a photon. The emitted photon will have energy equal to the difference between the levels of the impurity atom.

$$X^{+Z}(j) \rightarrow X^{+Z}(i) + h\nu \tag{2}$$

These two processes are sufficient to describe the coronal approximation where the sole populating mechanism is excitation from the ground state and the only depopulating method is radiative decay. The coronal approximation is valid in the low density limit of a plasma. The opposite limit is when collisions dominate over all other populating mechanisms and level populations are driven to the Local Thermodynamic Equilibrium (LTE) values.

* Corresponding author.
E-mail address: caj0026@auburn.edu (C.A. Johnson).

https://doi.org/10.1016/j.nme.2019.01.013
Received 8 August 2018; Received in revised form 21 December 2018; Accepted 11 January 2019

Consideration of all transition rates is required when densities are in between the two limits. This is referred to as the collisional radiative regime. The collisional radiative formalism covers all three regimes and is known as collisional radiative theory [1] where the excited state populations are solved as a coupled system of first order differential equations (rate equations), see Eq. (3). Fusion plasmas as well as many other experimental plasmas are in the collisional radiative regime and neither the coronal or LTE approximations are appropriate. Instead, a collisional radiative model must be used. Modeling collisional radiative processes are essential for transport modeling both in the edge and core of fusion plasma. Collisional radiative processes also play a large role in modeling plasma material interactions. The important role of atomic processes necessitates accurate modeling which will be detailed herein.

The following is the set of collisional radiative rate equations. To illustrate metastable resolved coefficients, we consider a system that has both ground and metastable states. Metastables are long lived states that can not electric dipole decay to any lower level. Two adjacent charge states and the excited states of the lower charge state are considered.

$$\begin{aligned}
\frac{dN_{\sigma_1}}{dt} &= -N_e\left(\sum_{j\neq 1} q^e_{1\to j} + S_1\right)N_1 + \sum_{j\neq 1}(A_{j\to 1} + N_e q_{j\to 1})N_j \\
&\quad + N_e \sum_k R_{\nu_k\to\sigma_1} N_{\nu_k} \\
\frac{dN_{\sigma_2}}{dt} &= -N_e\left(\sum_{j\neq 2} q^e_{2\to j} + S_2\right)N_2 + \sum_{j\neq 2}(A_{j\to 2} + N_e q_{j\to 2})N_j \\
&\quad + N_e \sum_k R_{\nu_k\to\sigma_2} N_{\nu_k} \\
\frac{dN_i}{dt} &= -N_e\left(\sum_{j\neq i} q^e_{i\to j} + S_i\right)N_i + \sum_{j\neq i}(A_{j\to i} + N_e q_{j\to i})N_j \\
&\quad + N_e \sum_k R_{\nu_k\to i} N_{\nu_k} \\
\frac{dN_{\nu_1}}{dt} &= N_e\left(\sum_j S_j N_j\right) - N_e N_{\nu_1}\sum_j R_{\nu_1\to j} \\
\frac{dN_{\nu_2}}{dt} &= N_e\left(\sum_j S_j N_j\right) - N_e N_{\nu_2}\sum_j R_{\nu_2\to j}
\end{aligned} \tag{3}$$

In the lower charge state, the ground is denoted by σ_1 and the metastable by σ_2. The excited levels of the lower charge state are described by i. The upper charge state ground is denoted by ν_1 and metastable by ν_2. The equations show the time evolution of both ground, metastable states, and excited states. Note that excited states do not have long life times and normally contain a small fraction of the total population.

In the quasistatic approximation of the GCR equations, the excited states are assumed to be in equilibrium with the ground and metastable states. Therefore, the rate of change of the population of these states can be set to zero ($dN_i/dt = 0$), in the quasistatic approximation. The system of equations, Eq. (3), can be represented in matrix form (see the ADAS 208 manual [6]). While the rate of change in the excited state populations can be set to zero, this is not true for the ground and metastable states. These ground and metastable populations can vary with time in the plasma. In addition, plasma conditions such as T_e and n_e can also change on time scales that are faster than the time required for these states to reach an equilibrium value.

The excited state populations can now be solved via a matrix inversion, with the ground and metastable states brought as unknowns to the right hand side, leading to the reduced collisional radiative Eq. (4).

$$\begin{bmatrix} N_3 \\ N_4 \\ \cdots \\ \cdots \\ N_n \end{bmatrix} = \begin{bmatrix} C_{33} & C_{34} & \ldots & \ldots & C_{3n} \\ C_{43} & C_{44} & \ldots & \ldots & C_{4n} \\ \cdots & \cdots & \cdots & \cdots & \cdots \\ \cdots & \cdots & \cdots & \cdots & \cdots \\ C_{n3} & C_{n4} & \ldots & \ldots & C_{nn} \end{bmatrix}^{-1} \times \begin{bmatrix} -C_{31}N_{\sigma_1} - C_{32}N_{\sigma_2} - R_3 N_{\nu_1} - R_3 N_{\nu_2} \\ -C_{41}N_{\sigma_1} - C_{42}N_{\sigma_2} - R_4 N_{\nu_1} - R_4 N_{\nu_2} \\ -\ldots-\ldots-\ldots \\ -\ldots-\ldots-\ldots \\ -C_{n1}N_{\sigma_1} - C_{n2}N_{\sigma_2} - R_n N_{\nu_1} - R_n N_{\nu_2} \end{bmatrix} \tag{4}$$

$$N_i = \sum_\sigma - N_\sigma \sum_j C'^{-1}_{ij} C_{j\sigma} + \sum_\nu N_\nu \sum_j C'^{-1}_{ij} R_{j\nu} \tag{5}$$

C' is defined as the reduced collisional radiative matrix. A choice now arises in the normalization of the population. In some cases, excited states can have significant populations. When significant populations exist in excited states, a normalization with respect to the total population is required instead of normalizing to the ground and metastable populations.

The excitation Photon Emissivity Coefficient (PEC) is defined as the population of a level multiplied by the spontaneous emission coefficient. The PEC can be thought of as a function of the driving ground metastable populations of adjacent ionization states. The PEC is then dependent on excitation, ionization, and recombination. This is related to the spectral line intensities, and in most cases, excitation processes dominates the PEC. Table 1 shows the PEC definition, for brevity only the excitation portion of the PEC is given, denoted with the superscript 'ex'.

2.2. GCR coefficients

Both ADAS and ColRadPy allow the user to choose levels that are defined in the code to be metastable. When a level is not chosen to be a metastable it is assumed to be an 'excited' state. Excited states are assumed to be in equilibrium population with the ground state which effectively sets dN/dt of the metastable to be zero (see Eq. (3)). Generally, for light impurity species there are very few or no metastable levels selected.

Once the excited populations have been determined, different derived coefficients can be defined that are convenient for plasma physics, particularly for impurity transport codes. The so called GCR coefficients as defined by Burgess and Summers [9] represent a way to sum the total possible ways for a process to occur. The same definitions for the GCR coefficients are used in this work and summarized in Table 1. The GCR coefficients assume Einstein summation over subscripts. A physical description of the GCRs can be helpful in interpreting the meaning behind them. For example, the total ionization from one charge state to the other is defined as the SCD. The total recombination from a charge state to the charge state of interest is defined as the ACD. The SCD and ACD give the rate of population transfer from one ionization state to an adjacent ionization state. The situation for systems with metastable

Table 1
GCR and derived coefficients.

Coefficient	Equation
$QCD_{\sigma\to\sigma'}$	$C_{\sigma'\sigma}$ - $C_{\sigma' j}C'^{-1}_{ji}C_{i\sigma}/N_e$
$SCD_{\sigma\to\nu}$	$S_{\nu\sigma} - S_{\nu j}C'^{-1}_{ji}C_{i\sigma}$
$ACD_{\nu\to\sigma}$	$r_{\sigma\nu} - C'^{-1}_{\sigma j}C_{ji}r_{i\nu}$
$XCD_{\nu\to\nu'}$	$N_e S_{\nu j}C'^{-1}_{ji}r_{i\nu'}$
PLT^{ex}_{σ}	$\Delta E_{ji}A_{j\to i}N^{ex}_j/N_\sigma$
$PEC^{ex}_{\sigma j\to i}$	$A_{j\to i}N^{ex}_j/N_\sigma$
$S/XB_{j\to i}$	SCD/PEC

states requires that the effective ionization and recombination rates be metastable resolved. In addition, it requires metastable cross coupling coefficients known as QCD and XCD coefficients. The QCD coefficient represents the transfer of population from one metastable state to another within the ionization state of interest and includes both direct population transfer between metastable states as well as the transfer via an intermediate excited state. The XCD coefficient represents the transfer of population between metastable states from the ionization stage just above the stage of interest. Populations in the upper ionization stage can recombine into the ionization state of interest from one metastable, redistribute through all the states and then ionize back into a different metastable state of the upper ionization state.

2.3. Determination of dominant populating mechanism

The GCR coefficients are the summation of all the pathways through all of the states. Each term in the summation can be used to evaluate the individual contributions to the population of a state. For instance, the intermediate level that populated a level of interest can be calculated by not carrying out the summation of Eq. (5). An example of these contributions applied to a neutral molybdenum system is detailed in Section 4. Similarly, the contributions of a level to the total ionization as well as recombination can be calculated.

3. Implementation of ColRadPy and comparison to ADAS

ColRadPy takes input files with effective collision strengths, ionization rates, recombination rates, and spontaneous emission coefficients. From these coefficients, the collisional radiative matrix is constructed. While not dependent on adf04 files [10], ColRadPy can read in this standard file format. The speed of ColRadPy allows for GCR coefficients and other quantities of interest to be calculated on the fly, allowing ionization balance calculations to be run directly from an ADAS adf04 input.

ColRadPy is capable of generating some basic atomic data such as Exchange Classical Impact Parameter (ECIP) ionization [9] and three-body recombination [11]. ECIP ionization rates can be made within ColRadPy by providing energy and level information for any level. ECIP is based on the work of Burgess [9]. Three body recombination is also calculated within ColRadPy using the collisional ionization rate coefficients and the detailed balance relation. ECIP is used when no fundamental ionization data is available for a given level.

ColRadPy is capable of handling an arbitrary number of metastables as well as a user-defined set of temperature and density grids. The NumPy linear algebra package [12] is used to invert the CR matrix. When possible, matrix operations are used to increase the speed of the code. All data related to the calculation is stored in a Python dictionary and is easily accessible.

ColRadPy results have been compared to ADAS [6] for C^{2+} to confirm validity of the code. C^{2+} was chosen because it has metastables in both C^{2+} and C^{3+} allowing all of the functionality to be tested with a small number of excited states included.

The ADAS data was downloaded from open-ADAS [10]. The population of individual levels has been confirmed to match ADAS over the tested parameter ranges. The GCR coefficients followed, matching over the tested parameter ranges. Both populations and GCR coefficients agreed to within numerical rounding errors for the parameter ranges tested.

ColRadPy is also capable of solving the full collisional radiative matrix time-dependently, ADAS is currently not capable of doing this. Time-dependence can be important for systems where there is significant population in many excited states or where ultra fast timescales need to be considered. Instead of the quasi-static approximation used in Eq. (4) where excited states are assumed to have no population change, the matrix is solved as a system of ordinary differential equations $n'(t) = An(t)$. The method used to solve the system of equations was adapted from R. LeVeque [13].

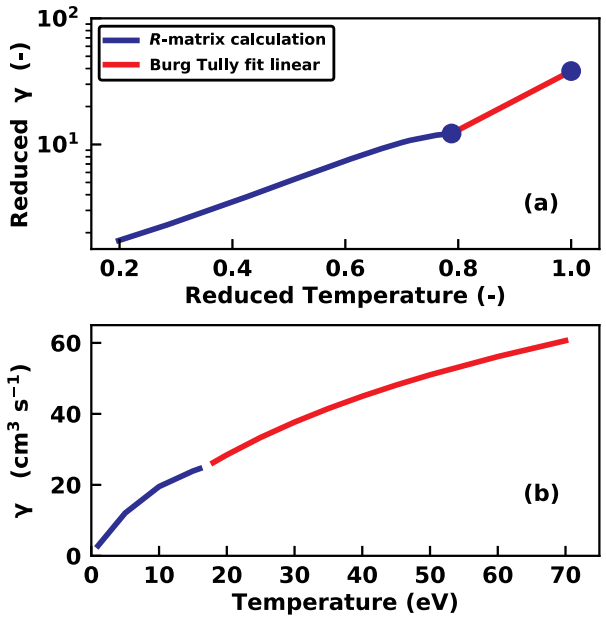

Fig. 1. Burgess–Tully effective collision strength extrapolation. (a) Effective collisional strengths for Mo I $4d^5 5s(^7S_3) \leftrightarrow 4d^5 5s(^5F_1)$ transition is in blue. Extrapolated Burgess–Tully fit in red. Last *R*-matrix calculated point and infinite energy point are the blue dots. (b) Effective collisional strength of the *R*-matrix calculation in blue and the extrapolated data in red. (For interpretation of the references to color in this figure legend, the reader is referred to the web version of this article.)

3.1. Extrapolation to higher temperatures

Extrapolation to temperatures higher than originally calculated from atomic codes can be accomplished with ColRadPy if the atomic data file includes limit points. This is achieved via the use of Burgess–Tully extrapolation [14]. The practical use of this will be discussed in Section 4.

As an illustration of ColRadPy, results will be presented for neutral molybdenum. Near neutral high-Z elements require more computational resources to calculate than previous low-Z elements due to the larger basis set that is required. The large basis sets do not allow calculations to be run up to high temperatures [15] and therefore require extrapolation to apply the calculation to possible divertor conditions where these near neutral systems exist. While extrapolation can be applied to any system where an infinite energy point was calculated, it is generally complex neutral systems that require this extrapolation. For example, the Mo neutral calculation was only calculated up to 17 eV. Divertor plasmas can produce temperatures much higher. Fig. 1 shows the extrapolation to higher temperatures for a transition between two neutral Mo levels $4d^5 5s(^7S_3)$ and $4d^5 5s(^5F_1)$. While the extrapolation can be carried out to infinite temperature, error in the extrapolation is reduced for temperatures closer to the last calculated value.

4. Example application of ColRadPy

A new Dirac *R*-matrix calculation for Mo I was recently completed and will serve as a test case for ColRadPy [16]. High-Z elements have a greater possibility of having a significant number of metastable states when compared to light elements. Metastables are those that are typically forbidden by electric dipole selection rules. Depopulating mechanisms are then limited to non-dipole radiative transitions (those that are relatively small) and electron impact excitation/de-excitation leading to a population build up in the metastables which can grow to a significant fraction of the ground state population. Neutral molybdenum has one metastable that has been investigated. However, if

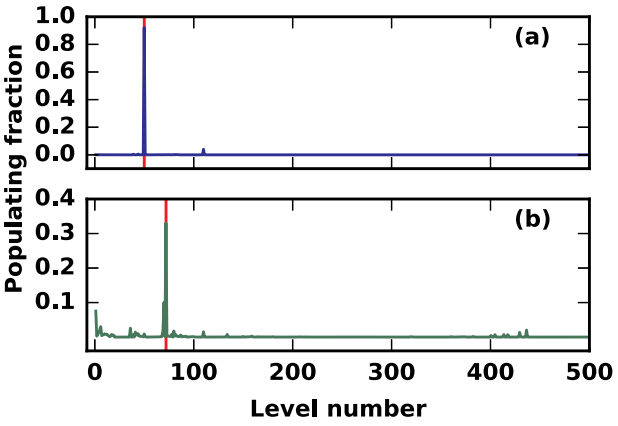

Fig. 2. Intermediate populating levels responsible for populating the neutral Mo $4d^5 5p(^7P_4)$ and $4d^5 5p(^5P_3)$ energy levels. These levels produce strong emission lines at 379.8 and 550.6 nm. The red vertical lines in each plot correspond to the ground state contribution, see discussion in Section 4. (a) Populating levels for $4d^5 5p(^7P_4)$, most of the population is being excited directly from the ground. (b) Populating levels for $4d^5 5p(^5P_3)$, a majority of the population is coming from other excited states and metastables. (For interpretation of the references to color in this figure legend, the reader is referred to the web version of this article.)

populations of 'excited' levels are investigated, there are many that have populations on the order of the first metastable. Excited states in light elements typically have less than 1×10^{-6} population. High-Z atoms can have many metastable levels which will require modeling to be carried out for each metastable. ColRadPy is capable of modeling an arbitrary number of metastable states. When metastable levels are present, the excited states become functions of both the ground and metastable populations. This means that the GCR coefficients as well as the derived coefficients are functions of the ground and metastable as well. When a ground state only calculation is carried out, it assumes that the metastable populations are in equilibrium with the ground state. If this is not the case, a metastable calculation must be completed using the non-equilibrium metastable fractions.

ColRadPy also allows the user to determine which intermediate levels populate a level of interest with Eq. (5) if the summation is not carried out. This allows one to see which levels in a calculation are important to modeling the spectral lines of interest. The Mo case study shows two interesting types of levels: those that are populated directly from the ground and those that are populated through intermediate steps as can be seen in Fig. 2. In the collisional radiative equations population starts in the ground state and then is distributed among other levels. The populating mechanism directly to the level of interest from the ground is seen as a spike at the number level of the level being investigated. For example, Fig. 2 (a) is level 50 which shows a large peak at level 50 corresponding to a large fraction of the population coming directly from the ground state. From Eq. (5), the term $C_{50,50} C^{-1}_{50,0} N_0$ will show up as a spike at level 50. Conversely, Fig. 2 (b) there is still a peak at level 71 corresponding to the ground directly populating level 71 and the significant fraction of populating mechanisms coming from other excited states are seen in the small peaks.

When viewing this kind of plot, it becomes obvious that some levels such as $4d^5 5p(^7P_4)$ (level 50) producing the 379.8 nm line can be modeled using only excitation from the ground and then a spontaneous emission down to the ground state. Plots of population fraction identify which transitions are required to accurately model spectral lines and make it possible to simplify complex systems such as high-Z near neutral systems.

ColRadPy is also able to preform an ionization balance in order to calculate time dependent changes in the metastable fraction as well as ionization states of elements.

4.1. Metastable influence on modeling high-Z atoms

Collisional radiative modeling is also required for accurate plasma transport modeling. A variety of transport codes from core to edge use collisional radiative modeling such as STRALH, ERO, UDEGE as well as many others [5,17]. Transport codes must track ionization states of impurity ions. In some cases, ionization states are 'bundled' together to reduce computational time [18]. Modeling metastable states may be required to accurately model low ionization states of high-Z atoms important for erosion measurements in fusion devices. Therefore, it is important to quantify if metastable states are important in the modeling of high-Z atoms.

From ColRadPy results, it is clear that there are potentially many levels in Mo I that have enough population to be considered a metastable state and is apparent with other high-Z atoms such as tungsten. Clearly, transport codes cannot feasibly consider more than a few metastable states. A trade off must then be made between accurately modeling the system and computational time. Many modeling codes cannot handle more than a few metastable states. For example, presently the ERO code can only model a ground state and one metastable for a given ionization state [19].

As mentioned above, the collisional radiative equation can be solved time dependently through the method of R. LeVeque [13]. When the equations are solved with this method, the quasistatic approximation is not assumed. Effectively every level is treated as metastable. The non-quasistatic solution can then be compared to the more widely used method solving the excited states as functions of the ground and metastable states while using a non-equilibrium ionization to get the time dependent population of the ground and metastable states.

A comparison can be made between the non-quasistatic solution and the more widely used method. For systems with no metastable states or very few (such as light systems), one would expect that the conventional method should reproduce the full solution once all metastable states have been accounted for in the ionization balance. Neutral beryllium was chosen as a case study because it is a light species with a metastable. Fig. 3 shows that the time dependent line intensity for the Be I line cannot be modeled accurately with just the ground. A metastable state is required in order for the quasistatic solution to accurately reproduce the non-quasistatic solution. Adding more than one metastable state does not significantly improve the conventional method because higher levels in Be I have small populations and have reached their steady state populations. Thus for Be I, one metastable is sufficient for accurate CR modeling.

Results for Be I are in contrast with the results for Mo I. Fig. 4 shows that the time dependent line intensity cannot be modeled accurately even with ten metastable states included. Lines that are populated significantly from metastable states (for example Mo I 379.8 nm) have two additional complications for heavy species. First, the metastable and ground can take a significant amount of time to reach equilibrium and therefore might need to be modeled time dependently. Metastables can have a significant contribution to the PEC intensity. The black dashed line in both (a) and (b) of Fig. 5 represents the sum of the contributions to the PECs from the ground and metastable in equilibrium. The solid color lines are the individual contributions to the PEC from both the ground and metastable. It is clear that in Fig. 5 (a), most of the contribution to the PEC comes from the ground state while in (b) there is a larger contribution to the PEC from the metastable level. The second complication is that a large number of excited states are not well described by the quasistatic approximation requiring a significant number to be modeled time dependently. In the case of Fig. 4, even 10 metastables are not sufficient to reproduce the results from the non-quasistatic CR model, see the difference between the red and black dashed lines. The use of bundling methods [20] may allow for closer reproduction of the full solution while maintaining a small number of metastables and will be investigated in the future. It is assumed that all the population starts in the ground state as opposed to some fraction of

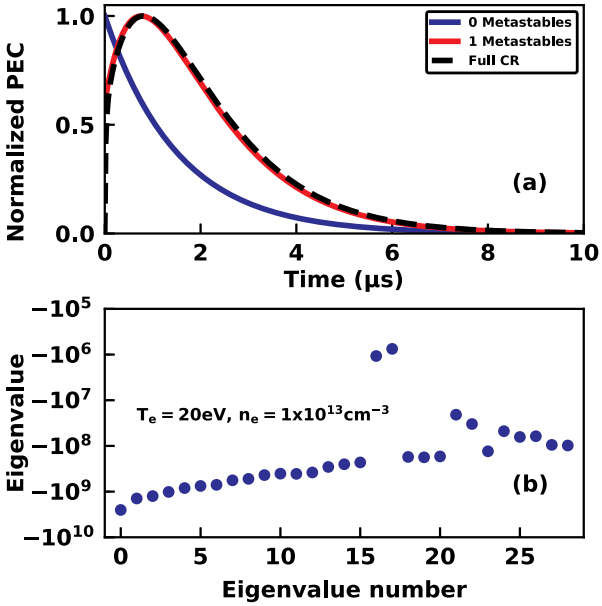

Fig. 3. Comparison of full time dependent and conventional solution for Be I at $T_e = 20$ eV, $n_e = 1 \times 10^{13}\,cm^{-3}$. (a) Non-quasistatic solution is illustrated by the black dashed line; conventional solutions with different numbers of metastable states are solid color lines. (b) Eigenvalues from the non-quasistatic solution. The ground and metastable states have markedly different values than the excited states and are represented by the two highest points in the figure.

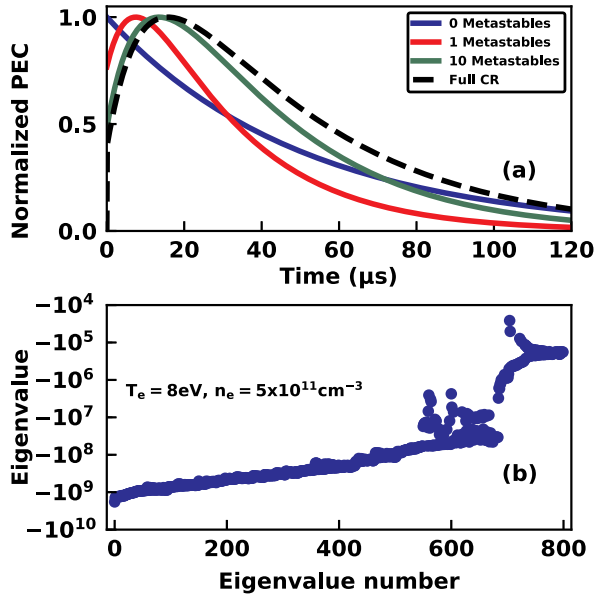

Fig. 4. Comparison of time dependent and conventional solutions for Mo I at $T_e = 8$ eV, $n_e = 5 \times 10^{11}\,cm^{-3}$. (a) Full solution is illustrated by the black dashed line. Conventional solutions with different numbers of metastable states are the solid color lines. (b) Eigenvalues from the non-quasistatic solution show a 'continuum' of decreasing values with no clear distinction between metastable and excited states as is seen for Be I.

the population beginning in a metastable state and requires that any atom eroded from a plasma facing material would come off the surface in its ground state. Experimental verification could be accomplished by observing spectral line emission near the plasma facing components. Experimental measurements from [21] suggest that most of the population starts in the ground state. Lines that are populated mostly from the ground should decay away from PFC as population is transferred from the ground to the metastable states. Spectral lines that are

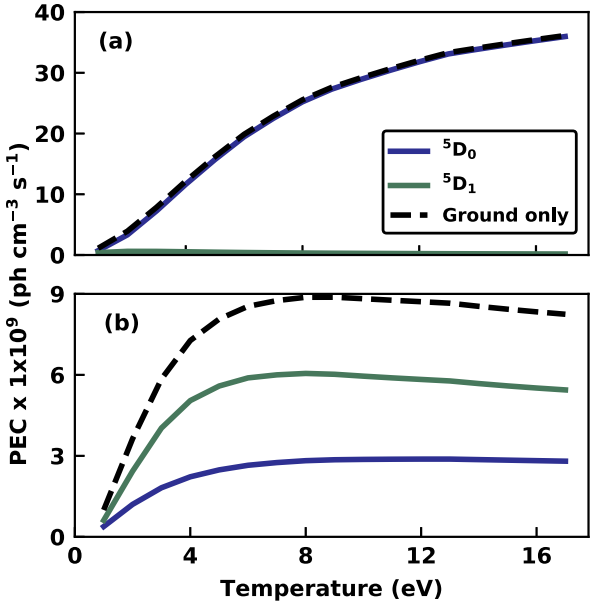

Fig. 5. Metastable resolved photon emissivity coefficient for Mo I 379.8 nm (a) and 550.6 nm (b). Ground state only calculation is illustrated by the dashed black line for each transition. Solid color lines blue and green are the ground state and first metastable level at their steady state equilibrium fraction. (For interpretation of the references to color in this figure legend, the reader is referred to the web version of this article.)

populated significantly from metastable states like those shown in Figs. 5 and 2 should peak in intensity at some time later than those populated directly from the ground as it takes some time to get collisional redistributed to the metastable state and populate the PEC.

5. Conclusions

The background of collisional radiative theory as well as the implementation of a new collisional radiative set of codes (ColRadPy) has been discussed. The flexible code allows for in-depth analysis of collisional radiative theory in addition to generating GCR coefficients for input into transport codes. The unique challenges of heavy species relevant for divertors in fusion devices are investigated. The large number of metastable states required to accurately model heavy species presents unique challenges both to CR modeling as well as plasma transport. A method to estimate important metastables is outlined and may serve to guide modeling efforts in the future.

Acknowledgments

This work is supported by the U.S. Department of Energy, Office of Science, Office of Fusion Energy Sciences, under award DE-SC0015877. Atomic data used for C and Be obtained from openADAS.

References

[1] D.R. Bates, A.E. Kingston, R.W.P. McWhirter, Recombination between electrons and atomic ions I. optically thin plasmas, Proc. R. Soc. Lond. 267 (1) (1962) 297–312 https://royalsocietypublishing.org/doi/abs/10.1098/rspa.1962.0101.

[2] H.P. Summers, W.J. Dickson, M.G. O'Mullane, N.R. Badnell, A.D. Whiteford, D.H. Brooks, J. Lang, S.D. Loch, D.C. Griffin, Ionization state, excited populations and emission of impurities in dynamic finite density plasmas: I. the generalized collisional-radiative model for light elements, Plasma Phys. Control. Fusion 48 (2) (2006) 263–293, https://doi.org/10.1088/0741-3335/48/2/007. URL http://arxiv.org/abs/astro-ph/0511561%0Ahttp://445 dx.doi.org/10.1088/0741-3335/48/2/007

[3] J.G. Doyle, H.P. Summers, P. Bryans, The effect of metastable level populations on the ionization fraction of Li-like ions, A&A 430 (2005) L29–L32, https://doi.org/10.1051/0004-6361:200400125.

[4] K. Behringer, H. Summers, B. Denne, M. Forrest, M. Stamp, Spectroscopic

determination of impurity influx from localized surfaces, Plasma Phys. Control. Fusion 31 (1989) 2059. URL http://iopscience.iop.org/0741-3335/31/14/001.
[5] R. Dux, STRAHL User Manual, (2006). IPP Report. https://pure.mpg.de/rest/items/item_2143869/component/file_2143868/content.
[6] H.P. Summers, The ADAS User Manual, version 2.2, http://www.adas.ac.uk/manual.php (2001).
[7] G. Del Zanna, K.P. Dere, P.R. Young, E. Landi, H.E. Mason, CHIANTI - An Atomic database for emission lines. Version 8, A&A 582 (2015) A56, https://doi.org/10.1051/0004-6361/201526827 arXiv:1508.07631.
[8] A.R. Foster, L. Ji, R.K. Smith, N.S. Brickhouse, Updated atomic data and calculations for X-ray spectroscopy, Astrophys. J. 756 (2) (2012), https://doi.org/10.1088/0004-637X/756/2/128 arXiv:arXiv:1207.0576v1.
[9] A. Burgess, H.P. Summers, The recombination and level populations of ions. I - hydrogen and hydrogenic ions, Mon. Not. R. Astron. Soc. 174 (1976) 345–391.
[10] Open adas(http://open.adas.ac.uk/), Accessed 5 January 2018.
[11] D. R. Bates, R. J. Moffett, Three-body recombination of positive and negative ions I. ions recombining in their parent gas, Proc. R. Soc. Lond. A Math. Phys. Sci. 291 (1424) (1966) 1–8.
[12] T.E. Oliphant, A guide to NumPy, Trelgol Publishing, USA, 2006 http://www.numpy.org/ , Online; accessed May 09, 2019.
[13] R. LeVeque, Finite difference methods for ordinary and partial differential equations: Steady-State and Time-Dependent Problems (Classics in Applied Mathematics Classics in Applied Mathemat), Soc. Ind. Appl. Math., Philadelphia, PA, USA, 2007.
[14] A. Burgess, J.A. Tully, On the analysis of collision strengths and rate coefficients, Astron. Astrophys. 254 (1991) 436–453.
[15] R.T. Smyth, C.P. Ballance, C.A. Ramsbottom, C.A. Johnson, D.A. Ennis, S.D. Loch, Dirac *R*-matrix calculations for the electron-impact excitation of neutral tungsten providing noninvasive diagnostics for magnetic confinement fusion, Phys. Rev. A 052705 (2018) 1–9, https://doi.org/10.1103/PhysRevA.97.052705.
[16] R.T. Smyth, C.A. Johnson, D.A. Ennis, S.D. Loch, C.A. Ramsbottom, C.P. Ballance, Relativistic *R*-matrix calculations for the electron-impact excitation of neutral molybdenum, Phys. Rev. A 042713 (2017) 1–7, https://doi.org/10.1103/PhysRevA.96.042713.
[17] D. Naujoks, R. Behrisch, J.P. Coad, L.C. De Kock, Material transport by erosion and redeposition on surface probes in the scrape-off layer of JET, Nucl. Fusion 33 (4) (1993) 581–590, https://doi.org/10.1088/0029-5515/33/4/I05.
[18] X. Bonnin, D. Coster, Full-tungsten plasma edge simulations with SOLPS, J. Nucl. Mater. 415 (1, Supplement) (2011) S488–S491, https://doi.org/10.1016/j.jnucmat.2010.10.041. Proceedings of the 19th International Conference on Plasma-Surface Interactions in Controlled Fusion, URL http://www.sciencedirect.com/science/article/pii/S0022311510006215
[19] D. Borodin, A. Kirschner, A. Kreter, V. Philipps, A. Pospieszczyk, R. Ding, R. Doerner, D. Nishijima, J. Yu, Modelling of Be transport in PSI experiments at PISCES-B, J. Nucl. Mater. 390–391 (1) (2009) 106–109, https://doi.org/10.1016/j.jnucmat.2009.01.128. URL https://doi.org/10.1016/j.jnucmat.2009.01.128
[20] H.P. Summers, N.R. Badnell, A.R. Foster, A. Giunta, F. Guzmán, L. Menchero, C.H. Nicholas, M.G. O'Mullane, A.D. Whiteford, A. Meigs, Modelling spectral emission from fusion plasmas, AIP Conf. Proc. 1438 (2012) 181–188, https://doi.org/10.1063/1.4707875.
[21] E. Marenkov, K. Gutorov, I. Sorokin, Radiation of high-Z atoms sputtered by plasma, Nucl. Instrum. Methods Phys. Res. Sect. B 436 (October) (2018) 257–262, https://doi.org/10.1016/j.nimb.2018.10.005. URL https://linkinghub.elsevier.com/retrieve/pii/S0168583X18305858